

PRELIMINARY DESIGN OF THE NRL MODIFIED BETATRON

J. Golden, J. Pasour, D. E. Pershing⁺, K. Smith*, F. Mako⁺, S. Slinker⁺,
F. Mora*, N. Orrick, R. Altes#, A. Fliflet[@], P. Champney[#], C. A. Kapetanakos
Naval Research Laboratory, Washington, D. C. 20375

Summary

The principal subsystems of the NRL Modified Betatron Accelerator (MBA) have been designed. These subsystems include the air-core magnets, the mechanical structure, the vacuum system, the injector accelerator, and the pulse power capacitor banks. The

MBA concept^{1,2} uses an applied toroidal magnetic field, B_θ (2-5 kG) to improve the stability and confinement of a multikiloamp e-beam. Trapping of an injected beam will result from varying the B_z by a few

Gauss during the first poloidal bounce period. Externally driven coils will compensate the diffusion of the self magnetic field to maintain equilibrium.

Introduction

Extensive theoretical analysis of the equilibrium and stability of the modified betatron accelerator has

been performed during the past two years²⁻⁶. As a result, design scaling laws have been compiled from which a consistent set of device parameters has been determined. A preliminary design for the principal subsystems is reported for an electron injection energy of 1-3 MeV, a circulating beam current of 1-5 kA, and an orbit radius of 1 m. The post-acceleration energy is 50 MeV.

The design includes the operation requirements of (1) low field errors, (2) parametric flexibility, (3) acceptable cost and (4) reasonable access to diagnostic ports and components requiring periodic maintenance. General features of the design include air core coils powered by capacitor banks, a stiff nonconducting structure, and large rectangular toroidal field (TF) coils providing high access to the high vacuum torus.

The application of a toroidal field for providing the high beam current equilibrium makes injection into the torus difficult. However, the large wall images of the beam in conjunction with the TF produce large poloidal drifts that can move the beam away from the

injection point in one revolution³. Because the equilibrium major radius of a high current beam is sensitive to the vertical field, a small change in B_z during the first poloidal bounce period can effect beam trapping. A set of fast coils can produce the ΔB_z capture field (CF).

Maintaining the high current equilibrium requires compensation for the decay of the beam induced return current in the chamber wall. This can be accomplished with an additional set of externally driven coils. Constraints are placed on the chamber wall material by the magnetic diffusion time and by the high vacuum required in the torus. Pressures of $< 10^{-8}$ Torr are required to limit background plasma generation and thus avoid the fast growing streaming and ion resonance instabilities.

Finally, the design of the MBA has been influenced

+ JAYCOR, Inc., Alexandria, VA.
* Sachs/ Freeman Associates, Bowie, MD.
Pulse Sciences, Inc., San Leandro, CA.
@ B-K Dynamics, Inc., Rockville, MD.

by the constraints on the acceleration time τ_{acc} . A short τ_{acc} reduces the time available for instability growth. However, the need for low field errors and field index errors requires that τ_{acc} be large enough to permit penetration of magnetic fields through the chamber walls. For the preliminary design, $\tau_{acc} \approx 3$ msec. The choice of wall materials, coil construction, acceleration time and injection parameters thus involved a set of compromises.

Schematic Plan View

A plan view of the MBA is shown in Figure 1. The structure is based on an equilateral triangle with truncated vertices. Twelve rectangular toroidal field (TF) coils are equally spaced azimuthally about the major (vertical, z) axis. Several circular vertical field (VF) coils are located within the TF coils (one is shown as an example). Nested within the VF coils is the dielectric vacuum chamber that has a conducting coating on its inner surface. The capture field (CF) and image compensation field (ICF) coils are located just outside the chamber wall. The chamber is located on the midplane ($z=0$), and the device has midplane symmetry.

Six toroidal segments comprise the vacuum chamber. Four of the segments have one large port that permits access on the midplane through a slot 10 cm high and 40 cm long. One of these ports connects to the injection accelerator. At least two of the large ports facing the vertical legs of the structure connect to a pumping line and pumping station.

VF and TF Coils

The coils and bus connections are shown schematically in Figure 2. The TF coil design premise is that field uniformity and reasonable access to the torus for maintenance and diagnostics are more important than minimizing the field energy. Field non-uniformity results because of the azimuthal discreteness of the coils and because of limited flux penetration of the coils conductors. Coaxial buswork is used to reduce additional contributions to the field errors. The TF coils are series connected to keep the current for the single turn coils $< 1/4$ MA. Multilam louvred low ohmic joints are used to minimize the series resistance and still allow low maintenance joints. The TF coils include 3 demountable joints that provide installation and maintenance access to the VF coils, the auxiliary coils, and the chamber. The TF capacitor bank comprises 144 capacitors and stores 3 MJ at 10 kV.

The VF coils comprise 18 single turn hoops that provide the correct field and index at the orbit and satisfy the betatron flux condition. Each coil is connected to a coaxial lead that is series connected to the VF buswork. The VF capacitor bank consists of 48 capacitors and stores 900 kJ at 15 kV. In addition to the main VF coils, there are three single turn trimmer coils in the VF coil circuit. One trimmer is located on the midplane and primarily effects a few percent change in the flux within the orbit. The other two trimmers are located directly above and

below the torus minor axis. The purpose of these two coils is to change the field index.

Structure

The loads on the structure result from the hoop stresses on the coils and from the overturning (tilting) force produced by the "VF" crossed with the current in the TF coils. The loads are typically

$\sim 10^2$ Nt/cm impulses that are proportional to $J(t) \times B(t)$. The main structural design problem has been maintaining precise coil positions during the pulse (instead of ultimate yield or structural efficiency).

The principal elements of the structure are (1) two triangular decks of high stiffness in r , θ , and z translations and rotations, (2) three legs, located at the vertices, that hold the decks in place against the tilt forces and hoop stresses, (3) a central tension bar, and (4) a central spline to hold the inward and twist forces on the inner vertical segments of the TF coils. In addition, vertical tension bars just radially outboard of the TF coils reduce the radial span of the loaded deck beams and provide additional support to the TF coils. The structure is non-conducting for the most part. The structural members are made of assemblies of polytruded epoxy-glas beams with electrically isolated stainless steel plates along selected flanges to enhance the product EI (where E = modulus of elasticity, and I = moment of inertia). The legs are made of aluminum.

Each major subassembly and the structure as a whole has been analyzed statically by analytic methods

and by a finite element method code (NASTRAN)⁷. A transient analysis has also been performed using NASTRAN. Predicted deformations during the pulse are below 3/4 mm at all places and below 1/2 mm in most locations.

CF and ICF Coils

Two auxiliary magnetic field coil systems are employed in addition to the VF and TF coils. These are the capture field (CF) and image compensation field (ICF) coils. The CF coils produce a B_z field inside the torus to move the beam equilibrium position away from the injector during the first poloidal bounce period. The ICF coils compensate for the self-field diffusion associated with the decay of the beam image currents.

There are 13 CF and 16 ICF coils mounted approximately 2.5 cm from the vacuum chamber at a radius of 19.5 cm from the toroidal minor axis. The coils are spaced 11.25° apart. There are no CF coils at $\phi = \pm 90^\circ$. Calculation of the magnetic fields has

been performed using TRIDIF⁸, a computer program that solves the diffusion equation for the vector potential, A_ϕ , and for the fields B_z , B_r . The diffusion

of the fields through a resistive vacuum wall (or the equivalent coating on the wall) has been included.

The CF coils are energized by a half-sine wave of 200-300 nsec risetime. The timing is chosen so that the CF peaks at injection and modifies the VF ($B_z \approx 150$ G) by 2-4 Gauss (see fig. 3). Ideally,

the CF should be a zero index field. After approximately one bounce period, the CF coils are clamped at zero current.

The ICF coils are energized during beam injection with an exponentially rising voltage pulse. The risetime is 1.5 μ sec. The L/R time of the ICF coils is ~ 5 μ sec and the diffusion time through the chamber and CF coils is comparable to the bounce period.

Approximately 6% of the flux diffuses out. At 3 μ sec after injection, the currents [ICF coils] are kept constant by a powered crowbar circuit.

The CF coils are driven with ~ 40 kV, and the current I_n in the coil at $\phi = \phi_n$ is $I_n = -33 \cos \phi_n (1 - A \cos \phi_n)$ amps, where $A = 0.08$ and ϕ is the poloidal angle. The ICF coils

require a peak voltage of $IR + L_{tot} \dot{I}$. The peak

inductive component is ~ 30 kV and the resistive voltage is < 4 kV and decays slowly during the acceleration time. The current in the ICF coil

at $\phi = \phi_n$ is given by $I_n = \frac{-I_b}{16} (1 - A \cos \phi_n)$.

Vacuum System

The vacuum requirement is a base pressure

$\sim 2 \times 10^{-8}$ Torr. This is derived from the need to avoid a substantial plasma background. Therefore the vacuum chamber materials have been selected for low desorption rate, a bake-out at $\sim 120^\circ\text{C}$, and the system has been designed for high conductance and high pump speeds.

The primary source of outgassing is likely to be the injection accelerator diode. Unless a more

favorable material is found (e.g., Polysil)⁹, the insulator in the diode will be polymethylmethacrylate. Because this material in vacuum produces copious amounts of water vapor, measures must be taken to reduce the associated gas load in the torus. Fortunately, the requirement that the injection port area be kept small to avoid unacceptably large eddy current perturbations also leads to a low conductance between the injector and the torus. Thus, differential pumping can be used so that the gas flow from the diode into the torus is acceptably low.

The chamber consists of a fused silica torus ($r_o = 100$ cm, $a = 16$ cm) made of 60° sectors. The main torus vacuum seals are Viton O-rings. The other joints will use metal seals. The pumping stations are electrically isolated from the torus. The pumping lines are 40 cm in diameter, approximately 1 meter in length, and end at a 25 cm diameter gate valve. One pumping station has a 3000 l/sec cryopump, and one station has a 2500 l/sec turbomolecular pump. An essential feature of the vacuum chamber is the conducting coating applied to the inner surface. This coating provides the electrostatic and initial magnetic boundary around the beam. The coating carries the return currents during a short period after injection. It must have a thickness much less than a skin depth for the various resistive modes. In addition, the thin coating must survive a beam dump on the wall.

An adequate coating is a $1/3$ μ m thick vacuum vapor deposited layer of inconel. Such a layer has a magnetic diffusion time ~ 150 nsec and a resistivity of ~ 125 $\mu\Omega$ -cm. A calculation of temperature rise for various beam energies between 2 MeV and 50 MeV at a

current density of 3 kA/cm² (normal incidence) indicates that the coating will survive. Shock loading and dendrite formation in the dielectric substrate appear to be within acceptable limits. However, the response of fused silica to e-beam deposition must be studied further.

Injection

Internal injection has been selected as the primary injection method. In this scheme, the diode cathode to which the high negative potential pulse is

applied is located inside the torus. The electrons are emitted on the B_θ field lines and are accelerated toward and pass through a thin foil anode that is at torus potential (i.e. near ground).

The injected pulse shape must satisfy stringent requirements. For the electrons to have the correct orbit radius, the electron energy must be matched to B_z . Therefore, the injection acceleration must

generate a reproducible, low ripple ($\Delta V/V < \pm 1\%$) flat-topped voltage pulse.

Internal injection offers the advantage of avoiding the beam propagation across the magnetic field lines. It may, however, pose some difficulties in addition to adversely affecting the background gas pressure. Most important of these is the field error that results from the porthole perturbation of the images. Therefore, it is desirable to make the port as small as possible. The minimum size is determined from the condition that excessive emission or breakdown does not occur along the cathode shank. Magnetic insulation by the TF and the diode self-field may help reduce such leakage currents.

The presence of the diode cathode in the torus presents another potential difficulty. One issue is the applied cathode potential during the fall time of the diode pulse. Because the B_z -matched, flat voltage portion of the injector pulse lasts i.e., 20 nsec, for one revolution around the major axis, the electrons in the front of the pulse will encounter the diode field during the finite fall time. Therefore, a fall time much shorter than the flat-top duration is desired.

External injection schemes are under consideration as alternatives that avoid the injection port opening. In external injection, the beam must be transported across the TF. Among the possibilities are (1) a current carrying plasma channel and (2) transport along a wire. For these injection methods to be feasible, the beam must reach the torus without a substantial velocity component that is transverse to the TF at the end of the channel.

Conclusions

All the major components of the preliminary design are compatible and consistent with the scaling laws. Refinement of the design must address simplification of the auxiliary coils, the effect of e-beam deposition on the vacuum chamber, field perturbation reduction for internal injection, and transverse velocity reduction for external injection.

References

1. P. Sprangle and C. A. Kapetanakos, J. Appl. Phys. 49, 1 (1978).
2. C. A. Kapetanakos, P. Sprangle, D. Chernin, S. J. Marsh and I. Haber, Memo Report 4905, NRL, Wash. DC (1982).
3. C. A. Kapetanakos, P. Sprangle, and S. J. Marsh, Phys. Rev. Lett. 49 741 (1982).
4. P. Sprangle, C. A. Kapetanakos, S. J. Marsh, Memo Report 4666, NRL, Wash., DC (1981).
5. D. Chernin, P. Sprangle, Part. Accel., 12 85 (1982).
6. D. Chernin, P. Sprangle, Part. Accel., 12 101 (1982).
7. NASA Structural Analysis Program, COSMIC, U. of GA, Athens, GA.
8. J. R. Freeman, J. Comp. Phys. 41 142 (1981).
9. D. Keefe, S. S. Rosenblum, Rept LBL-14341, LBL Berkeley, CA (1982).

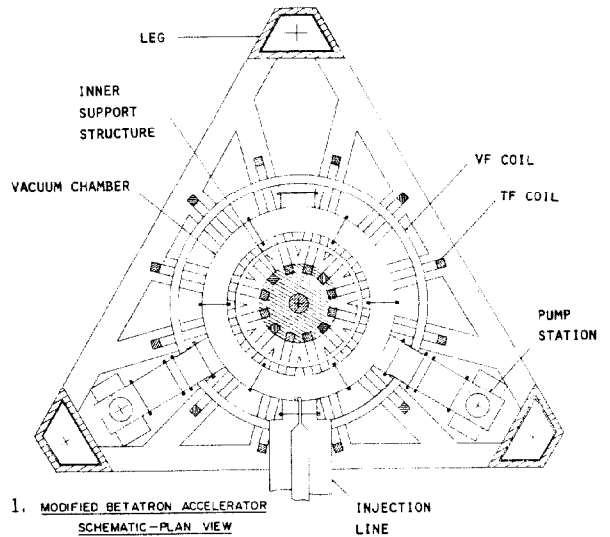


FIG. 1. MODIFIED BETATRON ACCELERATOR SCHEMATIC-PLAN VIEW

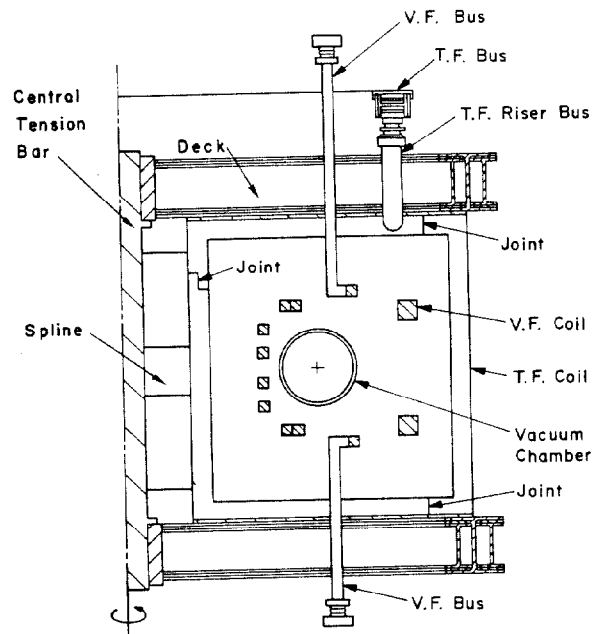


FIG. 2 Coils and Bus

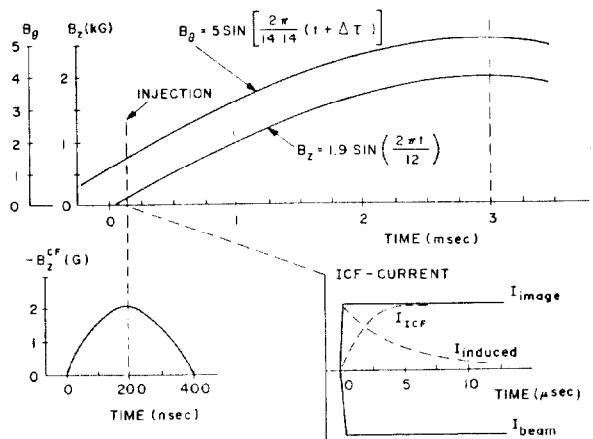


Fig. 3. Pulse Sequencing